

The Reason Why Sediment Transport is Analog to Sliding Friction

Thomas Pähtz^{1,2*} and Orencio Durán³

1. *Institute of Port, Coastal and Offshore Engineering,
Ocean College, Zhejiang University, 310058 Hangzhou, China*

2. *State Key Laboratory of Satellite Ocean Environment Dynamics,
Second Institute of Oceanography, 310012 Hangzhou, China*

3. *Department of Physical Sciences, Virginia Institute of Marine Sciences,
College of William and Mary, 23062 Virginia, USA*

Bagnold was the first to describe sediment transport in liquids and air by a constant friction coefficient at the bed surface. This is an essential, but poorly understood, assumption in many historical and modern theoretical attempts to derive expressions for the sediment transport rate. Using direct numerical simulations of sediment transport, we find, indeed, a constant friction coefficient at the bed surface for the entire range of parameters studied, including liquids and air. However, this does not result from a yield condition or inertial rheology, as previously suggested, but instead from a universal constraint on the average geometry of particle-bed rebounds in steady and homogeneous transport.

PACS numbers: 45.70.-n, 47.55.Kf, 92.40.Gc

Predicting the rate Q at which sediment is transported in liquids or air is a fundamental problem in Earth and planetary geomorphology [1–5]. Numerous experimental and theoretical studies have proposed analytical expressions for Q as function of fluid and particle parameters (e.g., [5–36]). Most of these expressions predict that Q is a power-law-like function of the excess shear stress, such as $Q \propto (\tau - \tau_t^r)^p$, where τ is the fluid shear stress and τ_t^r its extrapolated value at which Q would vanish.

In his pioneering studies, Bagnold [8–10] showed that such functional behaviors of Q can be derived when assuming that the transport layer ‘slides’ along the quasi-static sediment bed, which is characterized by a sliding friction law. That is, the friction coefficient μ , defined as the negative ratio between the particle shear stress P_{zx} and pressure P_{zz} ,

$$\mu = -\frac{P_{zx}}{P_{zz}} \quad (1)$$

is constant at the bed surface ($\mu_b = \text{const}$).

This assumption has later been adopted in analytical models of subaqueous sediment transport [12–15]. In analytical models of aeolian sediment transport, the same assumption has been used, though it was justified differently. There μ_b has been interpreted as an effective restitution coefficient characterizing the ratio between horizontal momentum loss and vertical momentum gain of particles rebounding at the sediment bed [31–36]. This interpretation assumes that contributions to the particle stress tensor from interparticle contacts (P_{ij}^c) are dominated by kinetic contributions from the transport of particles between contacts (P_{ij}^t), which implies $\mu \approx \mu^t = -P_{zx}^t/P_{zz}^t$.

Despite the widespread use of the sliding friction assumption, there is no clear understanding of its physical origin, its limits of application, nor how much the bed friction coefficient μ_b depends on the transport regime

(reported values range from 0.3 in water [17] to 1.0 in air [33]). Furthermore, μ_b is not well defined as there is no consensus on the location of the bed surface. Considering that μ can vary strongly around the bed surface, the absence of a precise definition makes it difficult to experimentally test this assumption.

Here we find, from direct numerical simulations of sediment transport in a Newtonian fluid, that a universal nearly-constant friction coefficient μ_b , at the effective location of particle-bed rebounds, follows from a universal constraint on the average rebound geometry in steady and homogeneous transport.

Technical definitions.—A local mass-weighted ensemble average of a quantity A at location $\mathbf{x} = (x, y, z)$ is defined as [37]

$$\langle A \rangle = \rho^{-1} \overline{\sum_n m^n A^n \delta(\mathbf{x} - \mathbf{x}^n)}, \quad (2)$$

where $\rho = \overline{\sum_n m^n \delta(\mathbf{x} - \mathbf{x}^n)}$ is the local particle mass density, m the particle mass, δ the delta distribution. Furthermore, the overbar denotes the ensemble average, and the superscript n refers to a quantity evaluated at the center of mass of particle n . Equation (2) is used to express the particle stress tensor as [37]

$$P_{ij} = P_{ij}^t + P_{ij}^c, \quad (3a)$$

$$P_{ij}^t = \rho \langle c_i c_j \rangle, \quad (3b)$$

$$P_{ij}^c = \frac{1}{2} \overline{\sum_{mn} F_j^{mn} (x_i^m - x_i^n) K(\mathbf{x}, \mathbf{x}^m, \mathbf{x}^n)}, \quad (3c)$$

where $K(\mathbf{x}, \mathbf{x}^m, \mathbf{x}^n) = \int_0^1 \delta(\mathbf{x} - s'(\mathbf{x}^m - \mathbf{x}^n) - \mathbf{x}^n) ds'$ is the ‘delta line’ connecting \mathbf{x}^m and \mathbf{x}^n , \mathbf{v} ($\mathbf{c} = \mathbf{v} - \langle \mathbf{v} \rangle$) the particle (fluctuation) velocity, and $\mathbf{F}^{mn} = -\mathbf{F}^{nm}$ the contact force applied on particle m by particle n ($\mathbf{F}^{mm} =$

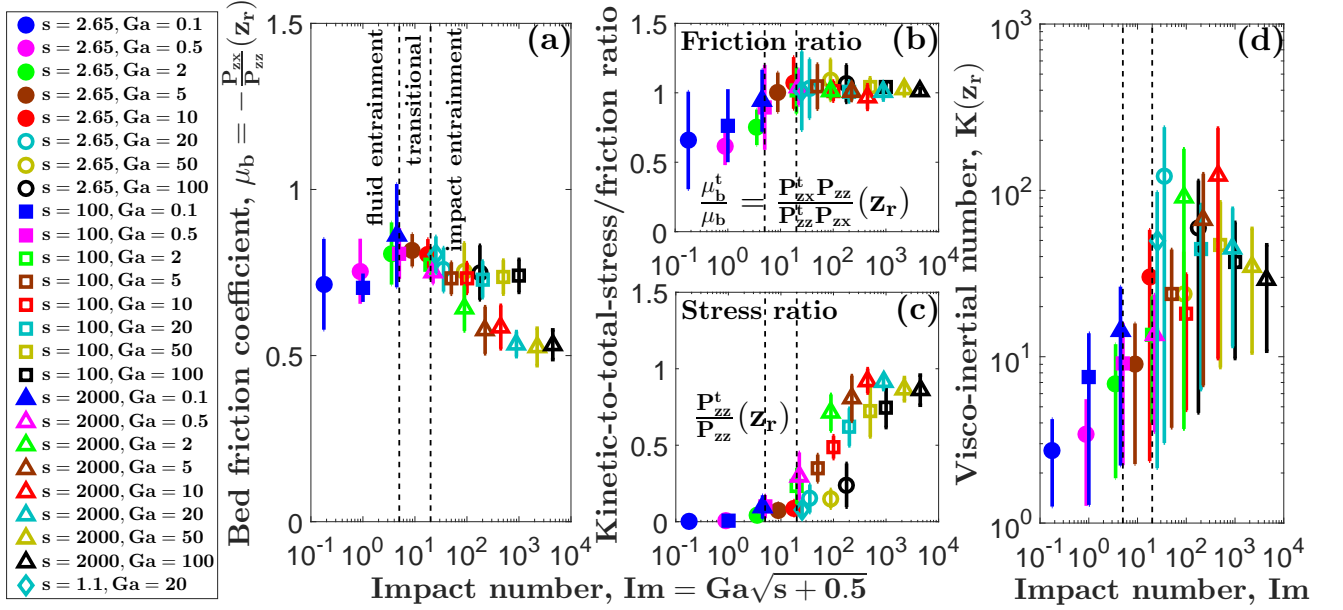


FIG. 1. **Constant friction coefficients.** (a) Friction coefficient μ , (b) ratio μ^t/μ between kinetic and total friction coefficient, (c) ratio P_{zz}^t/P_{zz} between kinetic and total bed particle stress, and (d) visco-inertial number K , all evaluated at the rebound location z_r , versus impact number Im for varying s and Ga . The vertical bars indicate the range of values these quantities cover when Θ is varied between $1-7\Theta_t^r$. The dashed lines indicate the bounds of transport regimes that are fully sustained by fluid entrainment ($Im \lesssim 5$) and impact entrainment ($Im \gtrsim 20$).

0). Moreover, Eq. (2) is used to define

$$L_{ij} = \rho \langle a_i^c v_j \rangle = \overline{\sum_n F_i^{cn} v_j \delta(\mathbf{x} - \mathbf{x}^n)}, \quad (4)$$

where \mathbf{a}^c is the total acceleration due to contact forces \mathbf{F}^c (i.e., $\mathbf{F}^{cn} = m^n \mathbf{a}^{cn} = \sum_m \mathbf{F}^{nm}$).

The tensor $L_{(ij)} = \frac{1}{2}(L_{ij} + L_{ji})$ is a measure for the average contact-induced rate of change of the kinetic energy tensor $\frac{1}{2}mv_i v_j$ per unit volume because $\frac{d}{dt} \frac{1}{2}mv_i v_j = m\dot{v}_i v_j$. The kinetic energy can change due to both conversion into other forms of energy (i.e., contact energy, rotational energy, sensible heat) and transfer from/to the contacting partner(s).

Finally, we introduce a collisional average of a quantity A , reading

$$\langle A \rangle^c = \frac{\langle |\mathbf{a}^c| |\mathbf{v}| A \rangle}{\langle |\mathbf{a}^c| |\mathbf{v}| \rangle} = \frac{\overline{\sum_n |\mathbf{F}^{cn}| |\mathbf{v}^n| A^n \delta(\mathbf{x} - \mathbf{x}^n)}}{\overline{\sum_n |\mathbf{F}^{cn}| |\mathbf{v}^n| \delta(\mathbf{x} - \mathbf{x}^n)}}. \quad (5)$$

Simulations.—The numerical model of Ref. [38], which couples a discrete element method for the particle motion and a continuum Reynolds-averaged description of hydrodynamics, has been shown to reproduce many observations concerning viscous and turbulent sediment transport in liquids and air [5, 38–41]. Using this model, we simulate steady, homogeneous sediment transport for particle-fluid density ratios $s = \rho_p/\rho_f$ within the range $s \in [1.1, 2000]$ and Galileo number $Ga = \sqrt{(s-1)gd^3}/\nu$

within the range $Ga \in [0.1, 100]$, where g is the gravity constant, d the mean particle diameter, and ν the kinematic viscosity. For each pair of s and Ga , we vary the dimensionless fluid shear stress (“Shields number” $\Theta = \tau/[(\rho_p - \rho_f)gd]$) between 1-7 times its threshold value $\Theta_t^r = \tau_t^r/[(\rho_p - \rho_f)gd]$. The simulated conditions, which include subaqueous ($s = 2.65$) and aeolian ($s = 2000$) transport, cover 5 orders of magnitude of the ‘impact number’ $Im = Ga\sqrt{s+0.5}$, which characterizes the mode of entrainment of bed sediment under threshold conditions [40]: $Im \lesssim 5$ when direct entrainment through fluid forces dominates, $Im \gtrsim 20$ when entrainment through particle-bed impacts dominates, and transitional behavior when $5 \lesssim Im \lesssim 20$. We would like to stress that, consistent with previous studies [40, 42], the restitution coefficient e for binary collisions only has a marginal influence on the results shown below for conditions with small s , indicating that lubrication forces are negligible.

Definition of bed surface.—We define the rebound location (bed surface) z_r as the elevation at which the collisional energy dissipation $P_{zz}\dot{\gamma}$ is maximal [40], where $\dot{\gamma} = d\langle v_x \rangle/dz$. $P_{zz}\dot{\gamma}$ always peaks near the bed surface due to an exponential increase of $\langle v_x \rangle$ with z in the upper layers of the sediment bed, which is associated with the transition from a quasi-static sediment bed to the mobile transport layer [40]. Indeed, a major portion of sediment transport occurs above z_r (Suppl. Mat. [43]).

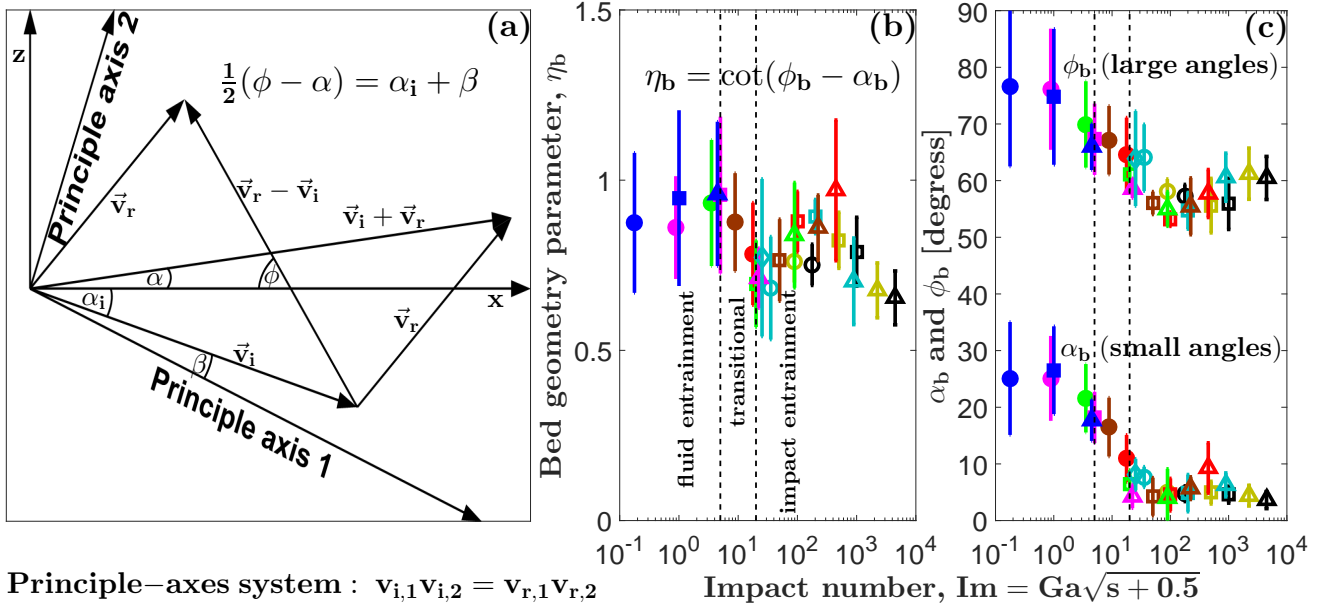


FIG. 2. **Particle-bed rebound geometry.** (a) Sketch of geometry of an average particle-bed rebound. (b) Geometry parameter η and (c) average contact force angle ϕ and average velocity angle α , all evaluated at the rebound location z_r , versus impact number Im for varying s and Ga . The vertical bars indicate the range of values these quantities cover when Θ is varied between $1-7\Theta_t$. The dashed lines indicate the bounds of transport regimes that are fully sustained by fluid entrainment ($Im \lesssim 5$) and impact entrainment ($Im \gtrsim 20$). For symbol legend, see Fig. 1.

Constant friction.—We find that the friction coefficient μ_b evaluated at the bed surface z_r is approximately constant for the entire range of simulated conditions (Fig. 1a). Surprisingly, the simulations also indicate that the kinetic and total friction coefficients are very similar ($\mu_b^t \approx \mu_b$) (Fig. 1b), even for those cases with negligible kinetic momentum flux ($P_{zz}^t(z_r) \ll P_{zz}(z_r)$), such as $s = 2.65$ and $Ga \geq 5$ (Fig. 1c). We would like to emphasize that arguments based on yield and/or a (visco)-inertial rheology [44–52] do not explain the constancy of μ_b as the visco-inertial number $K = \sqrt{(\rho_p d^2 \dot{\gamma}^2 + 2\rho_f \nu \dot{\gamma})/P_{zz}}$ [47, 48] varies over more than two orders of magnitude at z_r (Fig. 1d). Also, $K(z_r)$ is often much larger than order unity, which is about the upper boundary of the inertial granular flow regime.

Rebound geometry constraint.—We propose that the finding $\mu_b \approx \mu_b^t \approx \text{const}$ is instead a consequence of a constraint on the geometry of particle-bed rebounds. In order to express this constraint, we define a geometry parameter η and two angles ϕ and α as

$$\eta = \frac{L_{zz} - L_{xx}}{2L_{(xz)}} = \cot(\phi - \alpha), \quad (6)$$

$$\cot \phi = \frac{\sqrt{L_{(xz)}^2 - L_{xx}L_{zz}} - L_{(xz)}}{L_{zz}}, \quad (7)$$

$$\tan \alpha = \frac{L_{(xz)} - \sqrt{L_{(xz)}^2 - L_{xx}L_{zz}}}{L_{xx}}. \quad (8)$$

The angles ϕ and α are associated with the contact force angle ϕ^n of a particle n , defined through $\mathbf{F}^{cn}/|\mathbf{F}^{cn}| = -\cos \phi^n \mathbf{e}_x + \sin \phi^n \mathbf{e}_z$, and the velocity angle α^n , defined through $\mathbf{v}^n/|\mathbf{v}^n| = \cos \alpha^n \mathbf{e}_x + \sin \alpha^n \mathbf{e}_z$, respectively. In fact, when neglecting correlations arising from the average $\langle \cdot \rangle^c$ in Eq. (5), it follows $\alpha \approx \langle \alpha \rangle^c$ and $\phi \approx \langle \phi \rangle^c$ (Suppl. Mat. [43]). Since the averaging weight $|\mathbf{F}^{cn}||\mathbf{v}^n|$ strongly weighs towards energetic collisions, one may thus interpret ϕ and α as averages of ϕ_n and α_n over energetic collisions.

Near the bed surface, the most energetic collisions are particle-bed rebounds. Considering the average rebound of a single particle at the bed surface, with \mathbf{v}_i (\mathbf{v}_r) the average impact (rebound) velocity, it is possible to show that ϕ and α correspond to the angles depicted in Fig. 2a and $\frac{1}{2}(\phi - \alpha)$ to the average angle between the flow direction (x) and the first principle axis of the energy change rate tensor $\propto (\mathbf{v}_r \otimes \mathbf{v}_r - \mathbf{v}_i \otimes \mathbf{v}_i)$ (Suppl. Mat. [43]). Figure 2b shows that $\frac{1}{2}(\phi - \alpha)$ is strongly constrained in our direct transport simulations when evaluated at z_r as $\eta_b = \eta(z_r)$ exhibits an approximately constant value very close to μ_b (cf. Fig. 1a).

In contrast to η_b , both $\phi_b = \phi(z_r)$ and $\alpha_b = \alpha(z_r)$ show significant trends with the impact number (Fig. 2c). In particular, the data suggest a transition from large constant angles ($\phi_b \approx 75^\circ$, $\alpha_b \approx 25^\circ$) for sediment transport dominated by fluid entrainment ($Im \lesssim 5$) to small constant angles ($\phi_b \approx 55^\circ$, $\alpha_b \approx 5^\circ$) for sediment transport dominated by entrainment through particle-bed impacts

($\text{Im} \gtrsim 20$). This behavior of α_b illustrates the role of fluid drag for the vertical motion of particles. When vertical fluid drag can be neglected on average relative to other vertical forces (e.g., gravity, buoyancy, and added mass), steady transport requires $v_{rz}|_{z_r} \approx -v_{iz}|_{z_r}$ and thus $\alpha_b \approx 0$ (Fig. 2a). Otherwise, $v_{rz}|_{z_r}$ must be considerably larger than $-v_{iz}|_{z_r}$ to compensate the loss due to fluid drag.

Link to friction coefficient.— When kinetic momentum fluxes are dominant ($P_{ij}(z_r) \approx P_{ij}^t(z_r)$, typical for transport in air, cf. Fig. 1c), we get $\alpha_b \approx 0$ ($v_{rz}|_{z_r} \approx -v_{iz}|_{z_r}$) (Fig. 2c). Substituting into Eq. (6) within the particle-bed rebound framework depicted in Fig. 2a then yields $\eta_b \approx \mu_b^t$:

$$\eta_b = \cot \phi_b = -\frac{v_{r,x} - v_{i,x}}{v_{r,z} - v_{i,z}} \Big|_{z_r} = -\frac{v_{i,x}v_{i,z} + v_{r,x}v_{r,z}}{v_{i,z}^2 + v_{r,z}^2} \Big|_{z_r} \approx -\frac{\langle v_z v_x \rangle^c}{\langle v_z^2 \rangle^c} \Big|_{z_r} \approx -\frac{\langle v_z v_x \rangle}{\langle v_z^2 \rangle} \Big|_{z_r} = -\frac{P_{zx}^t}{P_{zz}^t} \Big|_{z_r} = \mu_b^t \approx \mu_b, \quad (9)$$

where the approximation $[\langle v_z v_x \rangle^c / \langle v_z^2 \rangle^c](z_r) \approx [\langle v_z v_x \rangle / \langle v_z^2 \rangle](z_r)$ is justified because there is a strong separation between slow particles of the bed surface and fast rebounding particles, which implies $[\rho_c \langle v_i v_j \rangle^c](z_r) \approx [\rho \langle v_i v_j \rangle](z_r)$, with ρ_c the mass density of fast particles.

When collisional momentum fluxes are dominant ($P_{ij}(z_r) \approx P_{ij}^c(z_r)$, typical for transport in liquids, cf. Fig. 1c), neglecting correlations between particle velocities and contact forces leads to $\eta_b \approx \mu_b^c$:

$$\eta_b = \frac{L_{zz} - L_{xx}}{L_{xz} + L_{zx}} \Big|_{z_r} \approx \frac{\langle a_z^c \rangle \langle v_z \rangle - \langle a_x^c \rangle \langle v_x \rangle}{\langle a_x^c \rangle \langle v_z \rangle + \langle a_z^c \rangle \langle v_x \rangle} \Big|_{z_r} = -\frac{\langle a_x^c \rangle}{\langle a_z^c \rangle} \Big|_{z_r} = -\frac{dP_{zx}^c/dz}{dP_{zz}^c/dz} \Big|_{z_r} \approx -\frac{P_{zx}^c}{P_{zz}^c} \Big|_{z_r} = \mu_b^c \approx \mu_b, \quad (10)$$

where we use mass and momentum conservation ($\langle v_z \rangle = 0$ and $\langle a_i^c \rangle = -dP_{zi}^c/dz$ [37]), and the fact that the dominating contribution to vertical gradients of both $-P_{zx}^c$ and P_{zz}^c comes from gradients of the collision probability $\sim (\rho/\rho_p)^2$ (i.e., $dP_{ij}^c/dz \propto P_{ij}^c \rho^{-2} d\rho^2/dz$), because $(\rho/\rho_p)^2$ changes much more strongly with z than any other potentially influencing quantity at and above the bed surface.

Conclusion.—In this Letter, we showed that sediment transport in an arbitrary Newtonian fluid can be successfully described by a universal nearly-constant sliding friction coefficient μ at the bed surface z_r , defined as the effective location of particle-bed rebounds, which provides a means toward a unified theory of sediment transport [41]. This apparent yield condition has a kinetic origin in particle-bed rebounds, regardless of the transport regime (bedload or saltation), and cannot be reduced to the inertial rheology of dense granular flows.

ACKNOWLEDGEMENTS

We acknowledge support from grant National Natural Science Foundation of China (No. 11550110179).

* 0012136@zju.edu.cn

- [1] L. C. van Rijn, *Principles of sediment transport in rivers, estuaries and coastal seas* (Aqua Publications, Amsterdam, 1993).
- [2] M. H. Garcia, *Sedimentation engineering: processes, measurements, modeling, and practice* (American Society of Civil Engineers, 2007).
- [3] J. F. Kok, E. J. R. Parteli, T. I. Michaels, and D. B. Karam, *Reports on Progress in Physics* **75**, 106901 (2012).
- [4] A. Valance, K. R. Rasmussen, A. Ould El Moutar, and P. Dupont, *Comptes Rendus Physique* **16**, 105 (2015).
- [5] O. Durán, P. Claudin, and B. Andreotti, *Aeolian Research* **3**, 243 (2011).
- [6] E. Meyer-Peter and R. Müller, in *Proceedings of the 2nd Meeting of the International Association for Hydraulic Structures Research* (IAHR, Stockholm, 1948).
- [7] H. A. Einstein, *The bed-load function for sediment transportation in open channel flows* (United States Department of Agriculture, Washington, 1950).
- [8] R. A. Bagnold, *Philosophical Transactions of the Royal Society London A* **249**, 235 (1956).
- [9] R. A. Bagnold, in *US Geological Survey Professional Paper 422-I* (1966).
- [10] R. A. Bagnold, *Proceedings of the Royal Society London Series A* **332**, 473 (1973).
- [11] M. S. Yalin, *Journal of the Hydraulic Division* **89**, 221 (1963).
- [12] K. Ashida and M. Michiue, in *Transactions of the Japan Society of Civil Engineers*, Vol. 206 (1972) pp. 59–69.
- [13] F. Engelund and J. Fredsøe, *Nordic Hydrology* **7**, 293 (1976).
- [14] A. Kovacs and G. Parker, *Journal of Fluid Mechanics* **267**, 153 (1994).
- [15] Y. Nino and M. Garcia, *Journal of Hydraulic Engineering* **124**, 1014 (1998).
- [16] Y. Nino, M. Garcia, and L. Ayala, *Water Resources Research* **30**, 1907 (1994).
- [17] Y. Nino and M. Garcia, *Hydrological Processes* **12**, 1197 (1998).
- [18] A. D. Abrahams and P. Gao, *Earth Surface Processes and Landforms* **31**, 910 (2006).
- [19] F. Charru, *Physics of Fluids* **18**, 121508 (2006).
- [20] E. Lajeunesse, L. Malverti, and F. Charru, *Journal of Geophysical Research* **115**, F04001 (2010).
- [21] R. Kawamura, in *Translated (1965) as University of California Hydraulics Engineering Laboratory Report HEL 2 Berkeley* (1951).
- [22] P. R. Owen, *Journal of Fluid Mechanics* **20**, 225 (1964).
- [23] R. J. Kind, *Atmospheric Environment* **10**, 219 (1976).
- [24] K. Lettau and H. H. Lettau, in *IES Report*, Vol. 101 (1978) pp. 110–147.
- [25] J. E. Ungar and P. K. Haff, *Sedimentology* **34**, 289 (1987).

- [26] M. Sørensen, *Acta Mechanica Supplementum* **1**, 67 (1991).
- [27] M. Sørensen, *Geomorphology* **59**, 53 (2004).
- [28] T. D. Ho, A. Valance, P. Dupont, and A. Ould El Mottar, *Physical Review Letters* **106**, 094501 (2011).
- [29] M. P. Almeida, J. S. Andrade, and H. J. Herrmann, *The European Physical Journal E* **22**, 195 (2007).
- [30] M. P. Almeida, E. J. R. Parteli, J. S. Andrade, and H. J. Herrmann, *Proceedings of the National Academy of Science* **105**, 6222 (2008).
- [31] G. Sauermann, K. Kroy, and H. J. Herrmann, *Physical Review E* **64**, 31305 (2001).
- [32] O. Durán and H. J. Herrmann, *Journal of Statistical Mechanics* **2006**, P07011 (2006).
- [33] T. Pähitz, J. F. Kok, and H. J. Herrmann, *New Journal of Physics* **14**, 043035 (2012).
- [34] M. Lämmel, D. Rings, and K. Kroy, *New Journal of Physics* **14**, 093037 (2012).
- [35] J. T. Jenkins and A. Valance, *Journal of Fluid Mechanics* **26**, 073301 (2014).
- [36] D. Berzi, J. T. Jenkins, and A. Valance, *Journal of Fluid Mechanics* **786**, 190 (2016).
- [37] T. Pähitz, O. Durán, T.-D. Ho, A. Valance, and J. F. Kok, *Physics of Fluids* **27**, 013303 (2015).
- [38] O. Durán, B. Andreotti, and P. Claudin, *Physics of Fluids* **24**, 103306 (2012).
- [39] O. Durán, B. Andreotti, and P. Claudin, *Advances in Geosciences* **37**, 73 (2014).
- [40] T. Pähitz and O. Durán, (2017), <https://arxiv.org/abs/1605.07306>.
- [41] T. Pähitz and O. Durán, (2017), <https://arxiv.org/abs/1602.07079>.
- [42] R. Maurin, J. Chauchat, B. Chareyre, and P. Frey, *Physics of Fluids* **27**, 113302 (2015).
- [43] See supplementary materials for technical details and additional information.
- [44] G. MiDi, *The European Physical Journal E* **14**, 341 (2004).
- [45] C. Cassar, M. Nicolas, and O. Pouliquen, *Physics of Fluids* **17**, 103301 (2005).
- [46] P. Jop, Y. Forterre, and O. Pouliquen, *Nature* **441**, 727 (2006).
- [47] M. Trulsson, B. Andreotti, and P. Claudin, *Physical Review Letters* **109**, 118305 (2012).
- [48] L. Amarsid, *Rhéologie des écoulements granulaires immergés dans un fluide visqueux*, Ph.D. thesis, University of Montpellier, Montpellier, France (2015), <https://tel.archives-ouvertes.fr/tel-01328026/>.
- [49] M. Houssais, C. P. Ortiz, D. J. Durian, and D. J. Jerolmack, *Nature Communications* **6**, 6527 (2015).
- [50] M. Houssais, C. P. Ortiz, D. J. Durian, and D. J. Jerolmack, *Physical Review E* **94**, 062609 (2016).
- [51] R. Maurin, J. Chauchat, and P. Frey, *Journal of Fluid Mechanics* **804**, 490 (2016).
- [52] M. Houssais and D. J. Jerolmack, *Geomorphology* **277**, 251 (2017).